Bearing Condition Monitoring via Multiple Instantaneous Frequency Path Extraction from Enhanced Time Frequency Representation

Rongmei Ding, Juanjuan Shi*, Jun Wang, Changqing Shen, Zhongkui Zhu
School of Rail Transportation, Soochow University,
Suzhou, 215131, China
jshi091@suda.edu.cn

***Abstract*—Short Time Fourier Transform (STFT) has been widely adopted for instantaneous frequency (IF) ridge extraction in bearing fault diagnosis under variable speeds. However, the readability of STFT-resulting time frequency representation (TFR) depends on how close the frequencies matching between the transforming bases and signal components. However, frequencies of STFT bases are time-invariant and thus do not match IFs of the vibration signal under variable speed conditions. Then, energy scattering may occur, resulting in IF ridge smearing on TFR for the multi-component vibration signal. To address this problem, transforming bases with time-varying frequencies are developed and a more energy concentrated TFR can be obtained. To get bases with time-varying frequencies, fast path optimization (FPO) is adopted to pre-estimate the IF of the analyzed signal. The TFR is then enhanced, from which multiple IF can be extracted and bearing health condition can be diagnosed. The effectiveness of the proposed approach is validated by experimental signals.**

Keywords-Bearing fault diagnosis; variablle speed condition; time frequency ridge exteaction; time frequency representation

I. INTRODUCTION

Time frequency representation (TFR) based instantaneous frequency (IF) extraction from the vibration signal is a popular technique based on linear transform for bearing fault diagnosis cases where the tachometer installation is not allowed due to the cost concerns and the design reason [1]. Short Time Fourier Transform (STFT), as a powerful time-frequency analysis approach, has been widely used to obtain the TFR of vibration signals [2]. However, the readability of TFR obtained by STFT can be greatly influenced by the frequency of the linear transform bases in addition to the window length [3]. The higher frequency agreement between the bases and signal components, the higher degree of the TFR energy concentration is. For constant speed condition, the matching can be easily satisfied due to the fixed bases frequencies of the STFT [4]. Nevertheless, as the frequencies of signals under time-varying speed operations are time-varying, it is difficult to match the frequencies of the linear transform bases with the frequencies of signal components. Thus, the applications of STFT are confined due to the undesirable time-frequency resolution [5].

Based on analysis presented above, this paper has proposed to develop bases with time-varying frequencies matching the frequencies of signal components under time-varying conditions. Firstly, IF ridges should be extracted from the traditional STFT-based TFR of the vibration signal. One of the simplest ridge extraction approaches is called "one-step" method, where a procedure is involved to locate an initial ridge point and then searching for the whole ridge point step by step following specific optimal functions [6]. Obviously, the IF extraction result is inaccurate once the initial ridge point is improperly picked. As such, the fast path optimization (FPO) algorithm [6,7] is utilized for the IF pre-extraction, named pre-IF, in this paper. Then, the time-varying frequency base strategy employs the extracted pre-IF to reset the frequencies of transforming bases so as to make the frequencies of bases and signal components matched and solve the smear problem in TFR.

The paper is organized as follows. Section 2 presents the FPO approach for the IF estimation and details of the time-varying frequency base strategy to enhance the readability of TFR. Section 3 gives the experimental examination and the paper is summarized in section 4.

II. THE PROPOSED METHOD

In this section, the introduction of the FPO is firstly elaborated and the pre-IF can then be estimated. Subsequently, the details of the strategy of bases with time-varying frequencies are introduced to post-process the TFR, leading to an enhancement to the TFR.

A. pre-IF estimation via FPO algorithm

STFT, as an important time frequency analysis method, is used to obtain the TFR in this paper. For a signal $x(t)$, it's STFT can be defined as [8]

$$X(\tau, f) = \int_{-\infty}^{+\infty} x(t) h(t-\tau) e^{-j2\pi ft} dt \qquad (1)$$

where $h(t)$ is the windowed function. $SP(\tau, f) = |X(\tau, f)|^2$ is

National Natural Science Foundation of China (51605319),
China Postdoctoral Science Fund (2017M611896).

the spectrum of the signal. Local maximum values of amplitudes at each time point on the TFR are calculated and the frequencies corresponding to local maximum values of amplitudes at the time point τ_n can then be obtained,

$$\begin{aligned} &f_m(\tau_n) = f, \\ &\left(d\left[X(\tau_n, f)\right]/df = 0 \middle\| d^2\left[X(\tau_n, f)\right]/df^2 < 0\right), m = 1,2,...,N_p \end{aligned} \tag{2}$$

where $\tau_n\,(n = 1,2,...,N)$ is time bins throughout the whole TFR, $N_p(\tau_n)$ is the number of local maximum values at τ_n, $f_m(\tau_n)$ is the m th peak at τ_n, whose amplitude can be denoted as $SP_m(\tau_n)$.

All the local peaks of amplitudes in the whole TFR are denoted by circles in the peak map, as Fig. 1 (a) shown. In order to extract an accurate pre-IF ridge, a FPO algorithm is adopted to determine which peak should be identified at every time bin. Frequency values corresponding to extracted peaks then constitutes the pre-IF estimation. The FPO algorithm can be expressed as [6]

$$\begin{aligned} &\left\{m_c(\tau_1),...,m_c(\tau_N)\right\} \\ &= \arg\max_{\{m_1,...,m_N\}} \sum_{n=1}^{N} F\left[\tau_n, SP_{m_n}(\tau_n), f_{m_n}(\tau_n), \left\{f_{m_1}(\tau_n),..., f_{m_n}(\tau_n)\right\}\right] \end{aligned} \tag{3}$$

where $m_c(\tau_n)$ determines the extracted peak at τ_n, $F[\ ]$ represents a support function for optimization. The support function is specifically formulated as

$$\begin{aligned} F[\ ] = &\log SP_m(\tau_n) + \omega_2\left(f_m(\tau_n), m[f_d], IQR[f_d], \alpha\right) \\ &+ \omega_1\left(f_m(\tau_n) - f_d(\tau_{n-1}), m[\Delta f_d], IQR[\Delta f_d], \beta\right) \end{aligned} \tag{4}$$

where

$$\begin{aligned} &\omega_1\left(f_m(\tau_n) - f_d(\tau_{n-1}), m[\Delta f_d], IQR[\Delta f_d], \alpha\right) \\ &= -\alpha\left|\frac{f_m(\tau_n) - f_d(\tau_{n-1}) - m[\Delta f_d]}{IQR[\Delta f_d]}\right| \end{aligned} \tag{5}$$

$$\omega_2\left(f_m(\tau_n), m[f_d], IQR[f_d], \beta\right) = -\beta\left|\frac{f_m(\tau_n) - m[f_d]}{IQR[f_d]}\right| \tag{6}$$

$$m[\ ] = perc_{0.5}[\ ], IQR[\ ] = perc_{0.75}[\ ] - perc_{0.25}[\ ] \tag{7}$$

where $f_d(\tau_{n-1})$ is the candidate frequency value at τ_n, Δf_d is the derivative of f_d, $perc_p[f(t)]$ is the p th Quantile of $f(t)$. Although the penalty parameters α and β can be tuned to match each specific case, ref. [6] has been demonstrated that α=β=1 is effective in most cases. Therefore, α=β=1 has been used in this paper. Solutions of the support function can then be given as [7][9]

$$\begin{aligned} &q(m, \tau_n) \\ &= \arg\max_k \left\{F\left[SP_m(\tau_n), f_m(\tau_n), f_k(\tau_{n-1})\right] + U(k, \tau_{n-1})\right\} \end{aligned} \tag{8}$$

$$\begin{aligned} U(m, \tau_n) &= F\left[SP_m(\tau_n), f_m(\tau_n), f_{q(m,\tau_n)}(\tau_{n-1})\right] \\ &= U\left(q(m, \tau_n), \tau_{n-1}\right) \end{aligned} \tag{9}$$

where $n = 1,2,...,N$ and $m = 1,2,...,N_p(\tau_n)$, $q(m, \tau_n)$ determines which peak value at the previous time bin τ_{n-1} should be linked with peaks at the current time bins $\tau_n\,(n = 2,...,N)$ and generate all possible paths, as shown in Fig. 1 (b). The $U(m, \tau_n)$ is an intermediate vector which is devoted to the optimization, i.e., picking the frequency value corresponding to the peak at time τ_N where $U(m, \tau_N)$ takes the maximum and the path corresponding to the picked frequency value at τ_N determined by $q(m, \tau_n)$ is extracted as the pre-IF ridge, as shown in Fig.1 (c).

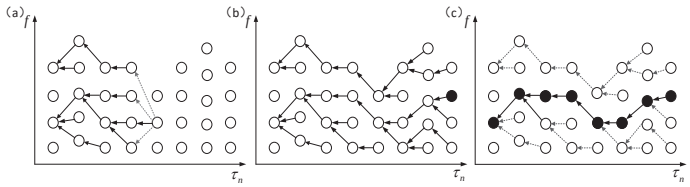

Fig. 1. Illustration of FPO algorithm: (a) local amplitude peaks, (b) all possible paths, (c) the optimization path (adopted from ref. [7])

Based on the above analysis, the FPO algorithm takes all local maximum values of amplitudes in the TFR into consideration and creates all possible optimization paths between amplitude peaks at previous and current moment, which ensures the continuity and accuracy of the IF ridge extraction.

B. TFR enhancement via developing transform bases with time-varying frequencies

Even though the pre-IF of the signal analyzed can be estimated by FPO algorithm, its accuracy is not always satisfactory. As displayed in Fig. 5 (d) and Fig. 8 (b), frequency jumps of pre-IF extracted from STFT resulting TFRs using FPO can be observed because STFT cannot provide a TFR free from smearing for non-stationary signal of multiple components. The underlying reason for smearing TFR from STFT is that the fixed frequencies of STFT bases cannot match the time-variant IF of the vibration signal under time-varying speed operations, as shown in Fig. 2 (a), thereby leading to scattering energy distribution of TFR. The IF ridges extracted from such TFRs often tend to be inaccurate.

Thus, the time-varying frequency base strategy is proposed in order to match the base frequencies of linear transform to the frequencies of signal component analyzed. With the linear transform bases whose frequencies match with the frequencies of vibration signal components, as shown in Fig. 2 (b), TFR of the signal can be post-processed

and its readability can be enhanced.

The Eq. (1) can be redefined as

$$X(\tau, f) = \int x_{win(\tau)}(t) G^{*}_{(\tau,f)}(t) dt \tag{10}$$

where $x_{win(\tau)}(t) = x(t)h(t-\tau)$ is the windowed signal, $G^{*}_{(\tau,f)}(t)$ is the novel linear transform kernel, expressed as

$$G^{*}_{(\tau,f)}(t) = \dot{l}_{(\tau,\alpha)}(t) \exp\left(-jfl_{(\tau,\alpha)}(t)\right) \tag{11}$$

where $l_{(\tau,\alpha)}(t) = 2\pi\left(t + \tan\alpha(t-\tau)^2/T\right)$ is the tangent line, $\dot{l}_{(\tau,\alpha)}(t)$ is the derivative of $l_{(\tau,\alpha)}(t)$, and $\alpha = \alpha(\tau) \in (-\pi/2, \pi/2)$ is the angle of linear transform bases, i.e., the inclined acute angle of the IF ridge in a window with '+' or '-' in the front. '-' indicates the acute angle between the IF path segment and the negative time axis direction and '+' indicates the acute angle between the IF path segment and the positive time axis direction. To realize the transform expressed in Eq. (10), the key is to obtain the acute angle $\alpha(\tau)$, which can be calculated using the extracted pre-IF. Then, the base with time-varying frequencies matching the IF of signal components can be obtained, as shown in Fig. 2 (b).

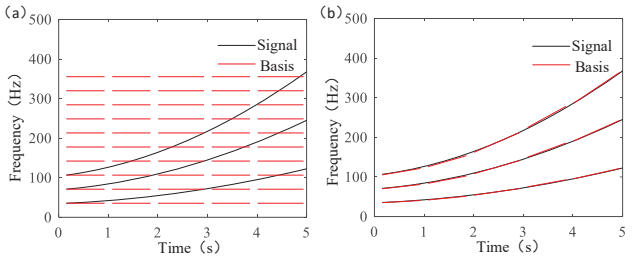

Fig. 2. Illustration of the time-varying frequency base: (a) time-invariant base frequencies, (b) time-varying base frequencies

With the novel linear transform bases where the frequency changing pattern in a window corresponds to the one of the IF ridge, the redefined STFT using Eq. (10) can be performed to generate a TFR with more concentrated energy, from which more accurate multiple IF path can then be extracted.

Obviously, the time-varying frequency base strategy utilizes the frequencies of the extracted pre-IF ridge obtained by FPO to realize the frequency matching between bases and signal components. The TFR is then enhanced, compared with STFT-resulting TFR. Based on the improved TFR, multiple IF paths can be extracted by the FPO algorithm to perform bearing fault diagnosis. To obtain multiple IF ridges associated with IFCF and shaft speed, frequency bands of the signal are segmented to obtain a lower frequency band and resonant frequency band. Shaft IF related IF ridges and IFCF related IF ridges can then be respectively extracted from the lower and resonant frequency band signals [10]. With the extracted IF curves, the bearing fault location can be diagnosed in the light of the ratio of any two IF paths from the lower frequency band and resonant frequency band signals, respectively.

The flow chart of the bearing condition monitoring under variable speed operations via multiple instantaneous frequency extraction based on the enhanced TFR is presented in Fig. 3.

III. Experimental Verification

Taking the vibrations of the bearing with an inner race fault as an example to examine the proposed approach, the experiment is conducted on a SpectraQuest Machinery Fault Simulator (MFK-PK5M), as shown in Fig. 4. Bearing parameters used in the test are given in Table I.

The raw vibration signal and its corresponding TFR are plotted in Figs. 5 (a) and (b), respectively, where no information related to inner race fault can be observed. To obtain IF ridges related to both shaft IF and IFCF, the signal is divided into the lower frequency band signal and the resonant frequency band signal. With the traditional STFT, the TFR of the lower frequency band signal can be obtained, as displayed in Fig. 5 (c). Two pre-IF ridges f_1 and f_2 extracted by FPO algorithm are presented in Fig. 5 (d). Due to that the energy scatters in the TFR of lower frequency band signal, the extracted pre-IF ridges present jumps in the interval of around 3 s to 5 s, which may influence bearing condition monitoring results. Thus, the time-varying frequency base strategy is applied to enhance the readability of the TFR. Then, the same IF extracted algorithm, i.e., FPO, is utilized to extract IF ridges.

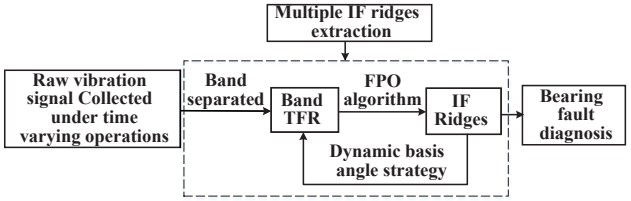

Fig. 3. The flowchart of multiple IF ridge extraction

TABLE I. Parameters of the Bearing Applied for Inner Race Fault Test

Bearing type	Number of balls	Pitch diameter	Ball diameter	FCF
ER16K	9	38.52 mm	7.94 mm	5.43×f_r

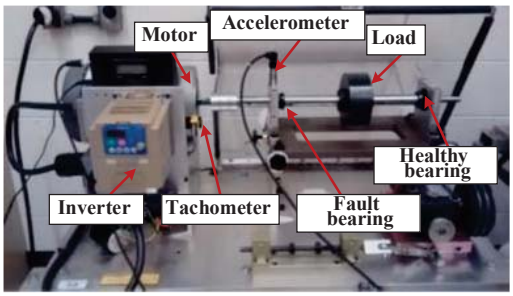

Fig. 4. Experimental setup

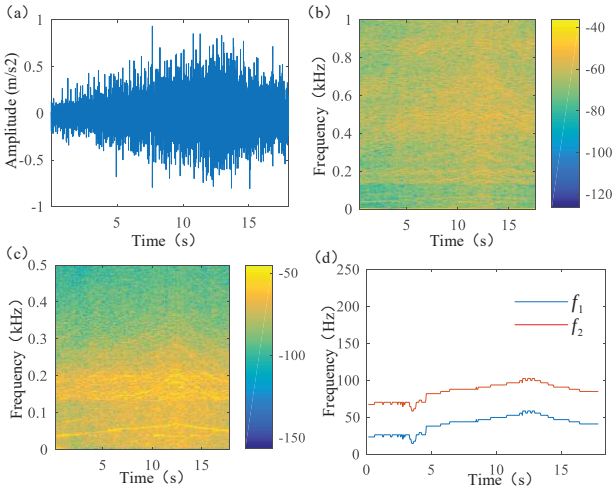

Fig. 5. Processing results of STFT. (a) Raw signal, (b) TFR of the raw vibration signal, (c) TFR of its lower frequency band, (d) Extracted IFs from lower frequency band using FPO algorithm

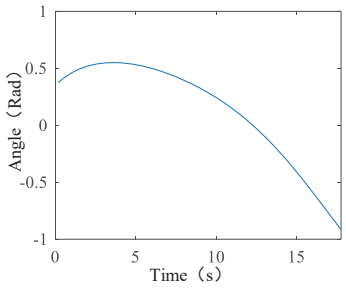

Fig. 6. The angle of the IF ridge (located in the very bottom)

Acute angles of tangent lines of IF ridge sections (truncated by windows) can be calculated based on the FPO-extracted pre-IF, as shown in Fig. 6, facilitating the new transform in Eq. (10). The resulting enhanced TFR is shown in Fig. 7 (a) and IF ridges $\overline{f_1}$ and $\overline{f_2}$ extracted by FPO from the enhanced TFR of lower frequency band signal can be observed in Fig. 7 (b).

TABLE II. MERS OF THE TWO EXTRACTED IF FROM LOWER FREQUENCY BAND

IF ridges	f_1	$\overline{f_1}$	f_2	$\overline{f_2}$
MRE	0.1839	0.0034	0.3126	0.2941

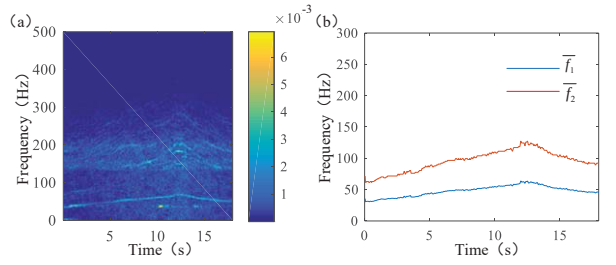

Fig. 7. Processing results of the proposed approach: (a) TFR of the lower frequency band, (b) Extracted IFs

Obviously, the frequency jumps in the interval 3 s to 5 s of the IFs have been eliminated, as can be observed in Fig. 7 (b). To quantitatively evaluate the enhancement, Mean Relative Error (MRE) is used. The MRE is computed by $1/m\sum_{i=1}^{m}\left|f_i - f_{real_i}\right|/f_{real_i}$, where f_i and f_{real_i} are the extracted IF value at time τ_i and the true frequency value at τ_i, respectively, m represents the number of the time instants. MREs of multiple IFs extracted by the FPO algorithm from traditional STFT-resulting TFRs and the enhanced TFRs of lower frequency band signal are listed in Table II. It can be seen that the MREs of the IF ridges $\overline{f_1}$ and $\overline{f_2}$ extracted from the enhanced TFR is less than these of the IF ridges extracted from the traditional STFT resulting TFR, indicating that the IF ridges from improved TFR are more accurate than the ones from STFT-resulting TFR.

The proposed strategy is also used to analyze the resonant frequency band signal. Figs. 8 (a) and (c) are the TFRs of resonant frequency band signal obtained by the traditional STFT and the proposed strategy, respectively. Figs. 8 (b) and (d) are the corresponding IF ridges extracted by the FPO algorithm, respectively. It can be clearly observed that the jumps presenting at the beginning of both IFs have been eliminated. The two IF ridges extracted from enhanced TFR are smooth without any sharp changes and fluctuations. Table III shows the MREs of the IF ridges from enhanced TFR and STFT-generating TFR. By observing Table III, it can be concluded that the time-varying frequency base strategy can improve the accuracy of the IF estimation. The MRE of the second IF ridge in the resonant frequency band signal is reduced by 64%.

Then, according to the ratios of any two points from lower frequency band signal and resonance frequency band signal in Fig. 8 (b) and (d), respectively, the bearing fault type can be diagnosed. As shown in Fig. 9, one can take a point from each IF ridge at the same time bin and then calculate the ratio of the point respectively from resonant frequency band signal to lower frequency band signal. The calculated ratios of points from IF ridge $\overline{f_3}$ and $\overline{f_1}$ equals 2.72 and the ratio of data points from $\overline{f_4}$ and $\overline{f_1}$ equals 5.65, almost identical to the half of the fault characteristic coefficient and the fault characteristic coefficient of inner race fault respectively. Thus, it can be concluded that the local bearing fault is positioned on the inner race of the bearing.

IV. CONCLUSION

For STFT-resulting TFR based multiple IF extraction and bearing health condition monitoring under time-varying speed conditions, one obstacle is the smearing problem of TFR due to that the fixed frequencies of transforming bases cannot match the frequency paths of signal components of vibrations. To address this problem, a time-varying frequency base strategy is proposed with the assistance of FPO algorithm which is applied to estimate the pre-IF ridges. Then, the inclined angle of IF ridge of each windowed signal can be calculated to make the base frequency match the IF

ridge of the windowed signal. The newly defined linear transform can subsequently be performed to enhance the readability of TFR. More accurate multiple IF ridges can be extracted from the enhanced TFR. The analysis results of experimental signal examine the effectiveness of the proposed method for the accurate IF ridge extraction and bearing health condition monitoring under variable speeds.

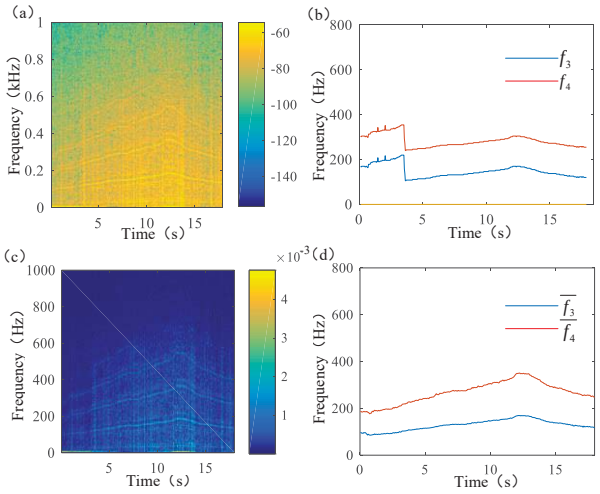

Fig. 8. Processing results for the resonance frequency band. (a) TFR obtained by the traditional STFT, (b) IFs extraction from the traditional STFT based TFR, (c) TFR obtained by the dynamic basis angle strategy, (d) IFs extraction from the proposed strategy based TFR

TABLE III. MERs OF TWO IF EXTRACTIONS FROM RESONANCE FREQUENCY BAND

IF ridges	f_3	$\overline{f_3}$	f_4	$\overline{f_4}$
MRE	0.0982	0.0898	0.0778	0.0281

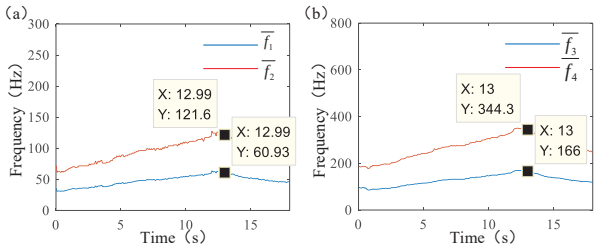

Fig. 9. Dynamic bases angle strategy based bearing fault diagnosis. (a) IFs extraction from the lower frequency band, (b) IFs extraction from the resonance frequency band

ACKNOWLEDGMENT

Authors are grateful for the Lab E026 of University of Ottawa for the data collection. Review comments from two anonymous reviewers are also very much appreciated, which is greatly helpful for us to improve the paper.

REFERENCES

[1] Z. Feng, X. Chen , and T. Wang . "Time-varying demodulation analysis for rolling bearing fault diagnosis under variable speed conditions." Journal of Sound and Vibration 400:71-85, 2017.

[2] J. Shi, Jiang X., et al. "Automatic instantaneous frequency order (IFO) extraction via integration strategy and multi-demodulation for bearing fault diagnosis under variable speed operation." Journal of Intelligent & Fuzzy Systems 34(6): 3547-3563, 2018.

[3] D. Gabor, "Theory of communication. Part 1: The analysis of information." Journal of the Institution of Electrical Engineers-Part III: Radio and Communication Engineering 93(26): 429-441, 1946.

[4] F. Millioz, and N. Martin. "Circularity of the STFT and spectral kurtosis for time-frequency segmentation in white Gaussian environment." IEEE Transactions on Signal Processing 59(2):515-524. 2011.

[5] Y. Guan, M. Liang, et al. "Velocity Synchronous Linear Chirplet Transform." IEEE Transactions on Industrial Electronics, 2018.

[6] D. Iatsenko, P. V. McClintock, et al. "Extraction of instantaneous frequencies from ridges in time–frequency representations of signals." Signal Processing 125: 290-303, 2016.

[7] H. Huang, N. Baddour, et al.. "Bearing fault diagnosis under unknown time-varying rotational speed conditions via multiple time-frequency curve extraction." Journal of Sound and Vibration 414: 43-60, 2018.

[8] E, Cabal-Yepez, A, G, Garcia-Ramirez, et al. "Reconfigurable monitoring system for time-frequency analysis on industrial equipment through STFT and DWT." IEEE Transactions on Industrial Informatics 9.2: 760-771, 2012.

[9] H. Huang, N. Baddour, et al. "Algorithm for multiple time-frequency curve extraction from time-frequency representation of vibration signals for bearing fault diagnosis under time-varying speed conditions." ASME 2017 International Design Engineering Technical Conferences and Computers and Information in Engineering Conference.

[10] C, Li, M. Liang, et al. “Time-frequency signal analysis for gearbox fault diagnosis using a generalized synchrosqueezing transform” Mech. Syst. Signal Process 26: 205-217, 2012.